the plant journal

SEB Society for Experimental Biology

*The Plant Journal* (2015) doi: 10.1111/tpj.12902

# CCR1, an enzyme required for lignin biosynthesis in Arabidopsis, mediates cell proliferation exit for leaf development

**Jingshi Xue, Dexian Luo[†], Deyang Xu[‡], Minhuan Zeng, Xiaofeng Cui, Laigeng Li and Hai Huang***

*National Laboratory of Plant Molecular Genetics, Shanghai Institute of Plant Physiology and Ecology, Shanghai Institutes for Biological Sciences, Chinese Academy of Sciences, 300 Fenglin Road, Shanghai 200032, China*

Received 19 May 2015; accepted 3 June 2015.
*For correspondence (e-mail hhuang@sibs.ac.cn).
[†]Present address: Biology Department, University of Massachusetts, Amherst, MA 01003, USA.
[‡]Present address: Department of Plant and Environmental Sciences, University of Copenhagen, DK-1871, Frederiksberg C, Denmark.

## SUMMARY

**After initiation, leaves first undergo rapid cell proliferation. During subsequent development, leaf cells gradually exit the proliferation phase and enter the expansion stage, following a basipetally ordered pattern starting at the leaf tip. The molecular mechanism directing this pattern of leaf development is as yet poorly understood. By genetic screening and characterization of Arabidopsis mutants defective in exit from cell proliferation, we show that the product of the *CINNAMOYL CoA REDUCTASE* (*CCR1*) gene, which is required for lignin biosynthesis, participates in the process of cell proliferation exit in leaves. *CCR1* is expressed basipetally in the leaf, and *ccr1* mutants exhibited multiple abnormalities, including increased cell proliferation. The *ccr1* phenotypes are not due to the reduced lignin content, but instead are due to the dramatically increased level of ferulic acid (FeA), an intermediate in lignin biosynthesis. FeA is known to have antioxidant activity, and the levels of reactive oxygen species (ROS) in *ccr1* were markedly reduced. We also characterized another double mutant in *CAFFEIC ACID O-METHYLTRANSFERASE* (*comt*) and *CAFFEOYL CoA 3-O-METHYLTRANSFERASE* (*ccoaomt*), in which the FeA level was dramatically reduced. Cell proliferation in *comt ccoaomt* leaves was decreased, accompanied by elevated ROS levels, and the mutant phenotypes were partially rescued by treatment with FeA or another antioxidant (*N*-acetyl-L-cysteine). Taken together, our results suggest that CCR1, FeA and ROS coordinate cell proliferation exit in normal leaf development.**

**Keywords: antioxidant activity, Arabidopsis, cinnamoyl CoA reductase 1, cell proliferation exit, ferulic acid, reactive oxygen species.**

## INTRODUCTION

The leaf is the major photosynthetic organ of most vascular plants. Leaf development in dicotyledons is usually thought to have three developmental phases: the proliferation phase, the expansion phase and the maturation phase (Beemster *et al.*, 2005). These three phases are not restricted spatially to specific or temporally to a precise developmental phase (Granier and Tardieu, 2009), but instead coexist showing a tip-to-base gradient, matching the leaf greening pattern (Donnelly *et al.*, 1999; Efroni *et al.*, 2010; Andriankaja *et al.*, 2012). Zones at the leaf tip shift earlier from one phase to another than those at the base (Poethig and Sussex, 1985). During the leaf expansion phase, cell division slows down and eventually stops, and cell expansion proceeds at a maximal rate to increase the individual cell area (Pyke and Leech, 1991; Donnelly *et al.*, 1999). Finally, in the maturation phase, tissue expansion slows down and ceases.

Studies exploring the molecular mechanism in phase changes in leaf development have made some important progress in recent years. *KLUH* (*KLU*), one of the many factors that promote cell proliferation in leaves, positively regulates a mobile growth factor, designated MGF, such that MGF is activated in the *KLU* expression domain and then diffuses homogenously throughout the leaf. Because of the restricted *KLU* expression domain after leaf growth, the reduced MGF levels cause the leaf cells to exit from the proliferation phase (Anastasiou *et al.*, 2007; Kazama *et al.*, 2010). Recent studies also found that repression of chloro-

plast development in leaves may result in a delay in cell proliferation exit, indicating that a retrograde signal from chloroplasts exists that may be involved in exit from the cell proliferation phase (Andriankaja *et al.*, 2012). However, until now, the nature of this putative chloroplast-produced signal has been largely unknown.

In this study, we report that cinnamoyl CoA reductase 1 (CCR1) is a key factor involved in progressive exit from the cell proliferation phase. CCR1 catalyzes the NADPH-dependent reduction of cinnamoyl CoA esters to their corresponding cinnamaldehydes, an important step in the biosynthesis of lignin monomers (Goffner *et al.*, 1994; Lacombe *et al.*, 1997; Piquemal *et al.*, 1998). Previous characterization of *ccr1* mutants showed that mutant plants not only contain less lignin in the interfascicular fibers and the xylem, but also have various developmental defects, including dwarf stature, reduced seed number, delayed plant senescence, and dramatically increased levels of ferulic acid (FeA) (Jones *et al.*, 2001; Derikvand *et al.*, 2008; Vanholme *et al.*, 2012).

In the present study, we show that *CCR1* is a developmentally regulated gene, whose basipetally ordered expression pattern perfectly matches that of exit from the cell proliferation phase during leaf development. In higher plants, FeA is an abundant phenolic cinnamic acid derivative that serves as a key intermediate in lignin biosynthesis (Boerjan *et al.*, 2003). FeA also has antioxidant activity both *in vitro* and in cells (Graf, 1992; Kanski *et al.*, 2002). We show that soluble FeA in leaf cells is closely negatively correlated with *CCR1* expression. As photosynthetic electron transport generates high levels of reactive oxygen species (ROS) (Foyer and Shigeoka, 2011) and oxidative stress terminates cell proliferation (Burdon, 1995; Boonstra and Post, 2004; Guo *et al.*, 2010; Tsukagoshi *et al.*, 2010), we propose that CCR1 acts through depletion of FeA to coordinate with ROS to direct exit from the cell proliferation phase during leaf development.

## RESULTS

### The *ccr1* mutation results in plants with increased cell proliferation

In the course of identifying factors that affect cell-cycle exit, we used ethyl methanesulfonate to mutagenize a previously characterized Arabidopsis mutant *asymmetric leaves1/2 enhancer7* (*ae7*), which shows defective cell proliferation (Yuan *et al.*, 2010; Luo *et al.*, 2012). We then screened for suppressors with impaired *ae7* phenotypes caused by a second mutation. *ae7* has reduced numbers of cells in the leaf and root. In the Landsberg *erecta* (L*er*) genetic background, leaves of *ae7* are pale green with serrated margins (Figure S1) (Yuan *et al.*, 2010; Luo *et al.*, 2012). Line 89/*ae7*, a plant identified from the $M_2$ progeny of the mutagenized *ae7*, showed compromised *ae7* phenotypes (Figure S1). This plant was backcrossed to wild-type L*er*, and a homozygous mutant that did not contain *ae7* was obtained from the segregating $F_2$ population. This mutant, designated line 89, showed a relatively small plant size, increased numbers of cells, and normal green leaves.

To identify the putative new gene, we crossed line 89 with wild-type Columbia-0 (Col-0), and used PCR-based genetic markers to analyze approximately 4000 recombinant chromosomes in individuals in the $F_2$ generation. The new gene locus was mapped to chromosome 1 between markers F7H2 and F3O9 (Figure S2). Sequencing of candidate genes in this region revealed that a previously characterized gene, *CCR1*, carried a C→T substitution in the third exon, resulting in an amino acid change from serine to phenylalanine (Figure S2). We then backcrossed line 89 with wild-type Col-0 another four times for further analysis. To confirm that the phenotypes of the back-crossed line 89 resulted from the *ccr1* mutation, we performed an allelism test by crossing line 89 (Col-0) with a previously identified *ccr1* mutant, *ccr1-g* (Col-0) (Derikvand *et al.*, 2008), and also performed a functional complementation test by introducing the $CCR1_{pro}$*:CCR1-GUS* construct into line 89 (Col-0). Both tests indicated that the phenotypes of line 89 (Col-0) were caused by the disrupted *CCR1* gene (Figure S2). The newly obtained mutant was renamed *ccr1-4*.

### Cells of *ccr1-4* remain in the mitotic state longer than wild-type cells

Similar to previously reported *ccr1* mutants, *ccr1-4* showed a relatively small plant stature (Figure 1a) and leaf size (Figure 1b). Further characterization of the *ccr1-4* phenotypes revealed that the palisade cells in the *ccr1-4* leaves were smaller (Figure 1d), while the number of cells per leaf was significantly greater (Figure 1f) compared with wild-type plants (Figure 1c,f). These phenotypes were also observed in leaves of the *ccr1-g* mutant (Figure S3). Similarly, the number of cortex cells in the root meristematic zone was greater in *ccr1-4* (Figure 1h,k,m) than in wild-type plants (Figure 1g,j,m). To understand whether the mutation affects the timing of cell differentiation, we performed a flow cytometric analysis to examine the nuclear ploidy of the *ccr1-4* mutant. Although the number of cells in the first leaves that had a 2C DNA content only slightly increased in *ccr1-4* compared with wild-type seedlings 9 days after germination, the decrease in the 2C cell ratio was much slower in *ccr1-4* than in wild-type from day 9 onwards (Figure 1o,p). In wild-type leaves, the number of 4C cells peaked on day 11, followed by a decrease in the ratio (Figure 1o), whereas the ratio of this population in the *ccr1-4* leaves reached its peak on day 23 (Figure 1p). The number of 8C cells in *ccr1-4* leaves increased much more slowly than in the wild-type, and 16C cells were barely detected in *ccr1-4* leaves during leaf development (Figure 1o,p). These

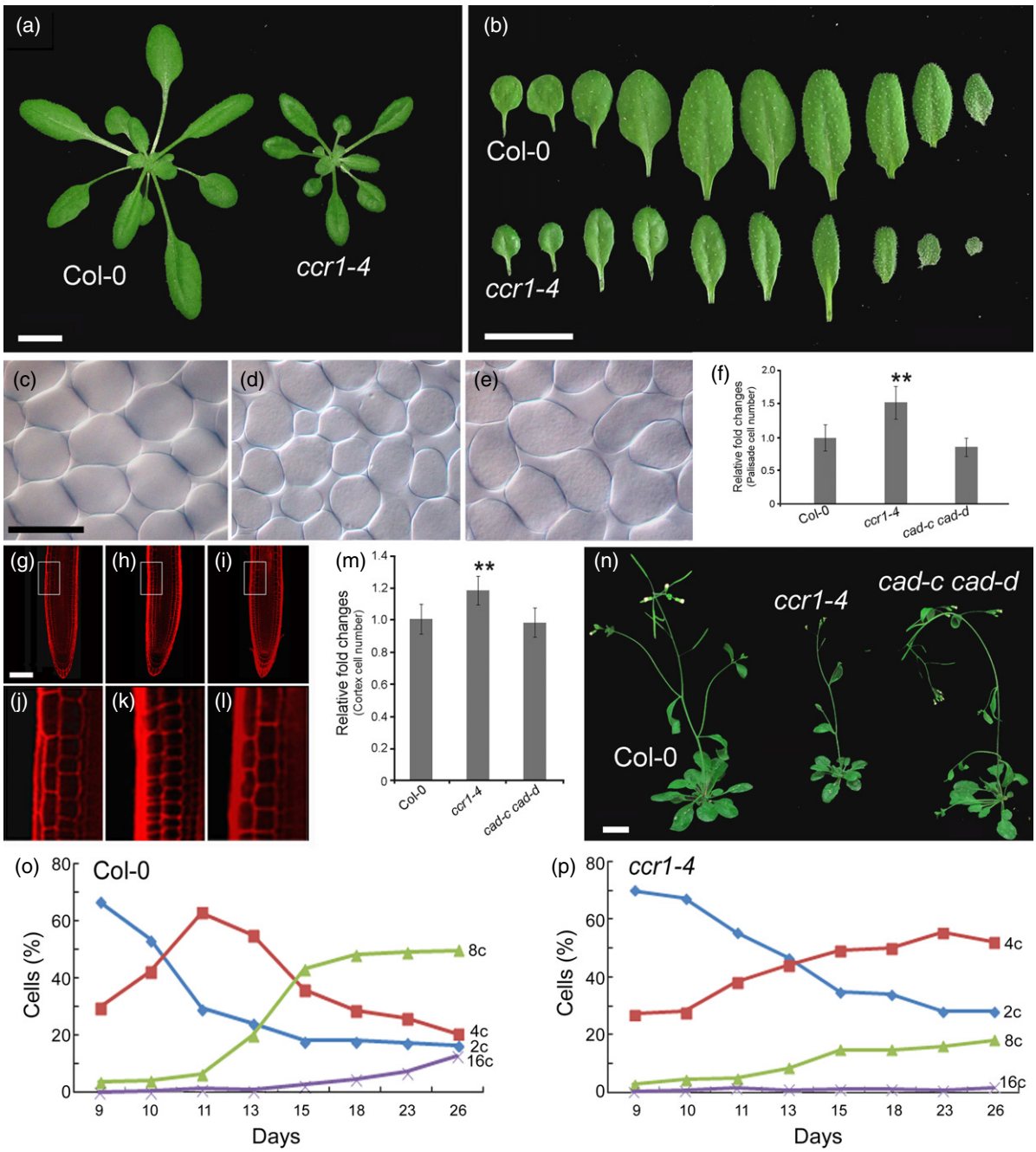


**Figure 1.** The *ccr1* mutation results in plants with increased cell number in leaves and roots.
(a) Plant sizes of 18-day-old wild-type Col-0 and *ccr1-4* mutant seedlings. Scale bar = 1 cm.
(b) Leaf sizes of 18-day-old wild-type and *ccr1-4* seedlings. Scale bar = 1 cm.
(c–e) Palisade cells of the first rosette leaves on day 25 from wild-type (c), *ccr1-4* (d) and *cad-c cad-d* (e) plants. Scale bar = 50 μm.
(f) Quantitative analysis of palisade cells. Cell numbers were increased in *ccr1-4* but not in *cad-c cad-d* leaves. The first leaves on day 25 were analyzed, and the value for cell number from wild-type Col-0 was arbitrarily fixed at 1.0.
(g–l) Laser scanning confocal microscopy to analyze the cell number in the cortex of roots of 7-day-old wild-type Col-0 (g, j), *ccr1-4* (h, k) and *cad-c cad-d* (i, l) seedlings. Scale bar = 100 μm (g); (h) and (i) are at the same magnification as (g), and (j), (k) and (l) are magnifications of the boxed regions in (g), (h) and (i), respectively.
(m) The *ccr1-4* mutant contained an increased number of cortex cells in the root meristematic zone, compared with wild-type and *cad-c cad-d* plants. Roots of 7-day-old seedlings were scored, and the value for cell number from wild-type Col-0 was arbitrarily fixed at 1.0.
(n) Stature of 30-day-old wild-type, *ccr1-4* and *cad-c cad-d* plants. Scale bar = 1 cm.
(o, p) Flow cytometry analysis to determine the nuclear ploidy of the first leaves of wild-type (o) and *ccr1-4* (p) at various times. Three biological replicates were performed and the results were consistent. The results shown are from one of the three experiments.
Values in (f) and (m) are means ± SD ($n$ = 10). Asterisks indicate statistically significant differences compared with Col-0 ($P < 0.01$).

results indicate that the *ccr1* mutation causes cells to retain their mitotic state for a prolonged time.

Cinnamyl alcohol dehydrogenase (CAD) is an NADPH-dependent reductase that converts cinnamaldehydes, the products of CCR1, into their corresponding alcohols (Luderitz and Grisebach, 1981). In Arabidopsis, two functionally redundant CAD members, CAD-C and CAD-D, catalyze this reaction. Like *ccr1*, the *cad-c cad-d* double mutant showed a decreased lignin content (Sibout, 2005). However, the double mutant plants showed normal growth (Figure 1n) and normal cell sizes in the leaf and root (Figure 1e,i,l). Also, the double mutant showed normal numbers of cells in the leaf and root cortex (Figure 1f,m), although the floral stem of *cad-c cad-d* was limp at maturity (Figure 1n). Thus, the *ccr1* and *cad-c cad-d* mutants showed similarly decreased lignin contents (Thevenin *et al.*, 2010), but only *ccr1* showed prominent developmental defects. Therefore, the *ccr1-4* phenotypes are probably caused by factors other than the decreased lignin content.

### *CCR1* expression is developmentally regulated in leaves

To understand how CCR1 affects cell proliferation, we analyzed the expression pattern of *CCR1* during leaf development. Because introduction of $CCR1_{pro}$*:CCR1-GUS* into *ccr1-4* fully rescued the *ccr1-4* phenotypes (Figure S2), we examined GUS staining in the first leaf of $CCR1_{pro}$*:CCR1-GUS*/*ccr1-4* plants. A total of five independent transgenic lines were examined, and they showed consistent GUS staining patterns. GUS staining first appeared at the leaf tip of seedlings on day 7 (Figure 2a), and then extended to the more proximal portion by day 9 (Figure 2b). The third or younger leaves of seedlings on days 7 and 9 were barely stained (Figure 2a,b, arrowheads). GUS staining covered the entire first leaf from day 11 onwards

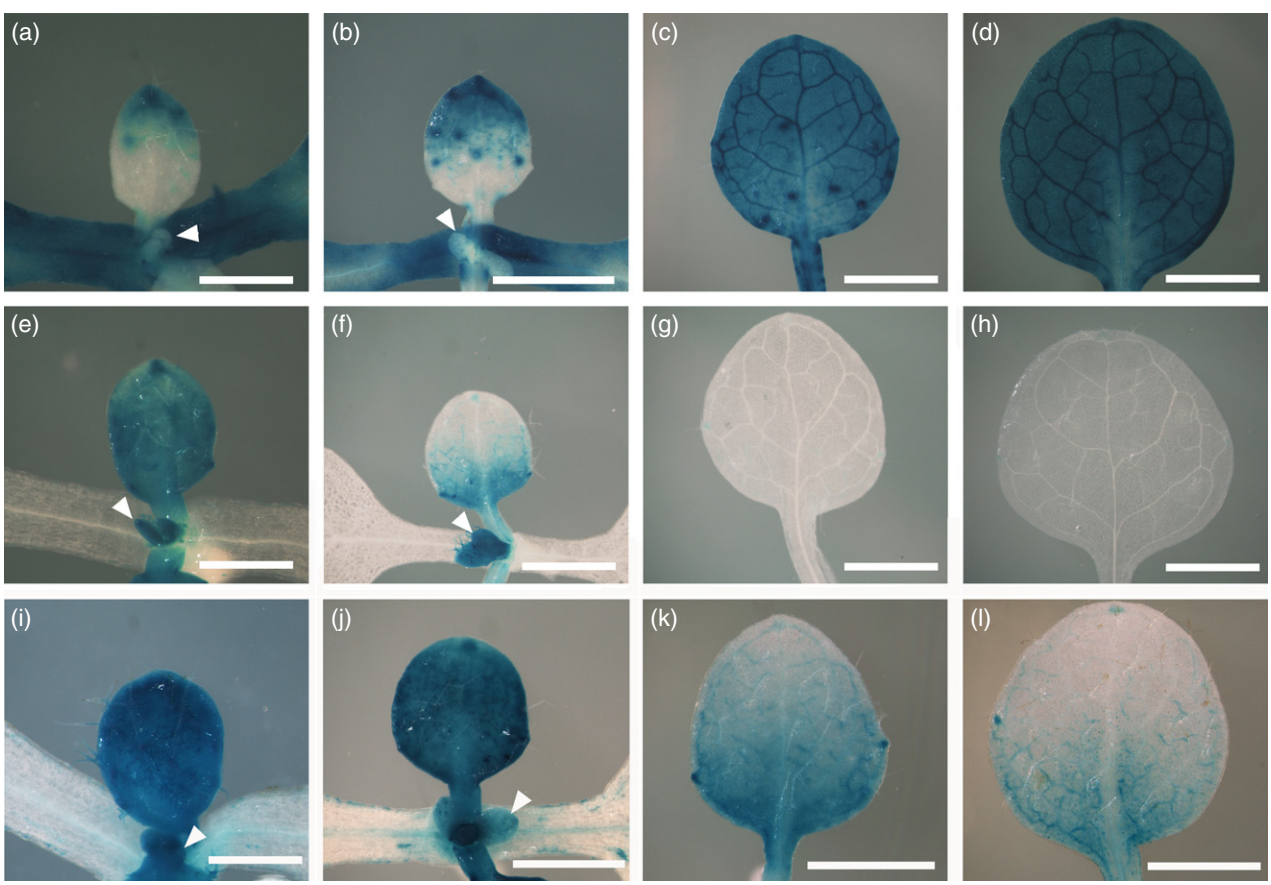


**Figure 2.** *CCR1* expression is developmentally regulated.
(a–d) *CCR1* expression patterns in developing leaves. $CCR1_{pro}$*:CCR1-GUS* was introduced into the *ccr1-4* mutant, and the first rosette leaves of a fully rescued mutant plant were analyzed on days 7 (a), 9 (b), 11 (c) and 13 (d). The arrowheads in (a) and (b) indicate the third or fourth leaves, which were barely stained.
(e–h) *CYCB1;1* expression patterns during leaf development in wild-type plants. GUS staining was analyzed in the first leaves of a $CYCB1;1_{pro}$*:Dbox-GUS*/Col-0 line on days 7 (e), 9 (f), 11 (g) and 13 (h).
(i–l) *CYCB1;1* expression patterns in *ccr1-4* leaves. GUS staining was analyzed in the first leaves of a $CYCB1;1_{pro}$*:Dbox-GUS*/*ccr1-4* line on days 7 (i), 9 (j), 11 (k) and 13 (l). The *ccr1* mutation resulted in leaves with a prolonged time for GUS signals to become detectable.
Arrowheads in (e), (f), (i) and (j) indicate the third or fourth leaves. Staining for all leaf samples was performed under the same conditions. The punctate GUS signals represent trichomes that may be stained at certain developmental stages. Scale bars = 0.5 mm (a, e, i) and 1 mm (b–d, f–h, j–l).

(Figure 2c,d). All these results indicate that *CCR1* expression in leaves is developmentally regulated.

Expression of *CYCB1;1* was shown to be a marker for dividing cells (Jacqmard *et al.*, 1999; Dewitte and Murray, 2003). Interestingly, the staining region of CYCB1;1pro:Dbox-GUS in a ccr1-4 leaf was nearly complementary to that of CCR1pro:CCR1-GUS. The third leaf or younger leaves of seedlings on days 7 and 9 were deeply stained (Figure 2e,f, arrowheads). *CYCB1;1*$_{pro}$*:Dbox-GUS* staining was weak at the distal region of the first leaves on day 7, then visible only in the middle and proximal regions on day 9 (Figure 2e,f), and no GUS staining was detected in leaves from day 11 onwards (Figure 2g,h). These results indicate that *CCR1* expression is coincident with exit from the cell cycle during leaf development.

We next analyzed *CYCB1;1* promoter activity in *ccr1-4* leaves using *CYCB1;1*$_{pro}$*:Dbox-GUS*/*ccr1-4* plants, which were obtained by introgressing the *CYCB1;1*$_{pro}$*:Dbox-GUS* construct into the *ccr1-4* mutant. On day 7, GUS staining was weak at the leaf tip of the first leaf of the wild-type (Figure 2e), but strong at the leaf tip of the first leaf of *ccr1-4* (Figure 2i). On day 9, GUS staining was weak or absent from the most distal part of wild-type leaves (Figure 2f), but still relatively strong in the whole leaf of *ccr1-4*, except for the tip (Figure 2j). On days 11 and 13, GUS staining was hardly detected in wild-type leaves (Figure 2g,h), but was detectable in *ccr1-4* leaves (Figure 2k,l). These results are consistent with the observation that the *ccr1* mutation results in a prolonged duration of cell proliferation in leaves (Figure 1p).

To understand whether exit from the cell proliferation phase in other plant tissues is also correlated with *CCR1* expression, we analyzed roots. In contrast to leaves, where dividing cells were usually not associated with *CCR1* expression, *CCR1* is expressed in dividing root cells, as root cells in the apical meristematic zone of *CCR1*$_{pro}$*:CCR1-GUS*/*ccr1-4* plants showed GUS staining (Figure S4). The vascular cylinder had the strongest GUS staining compared with the other parts of the root, whereas the root cap was barely stained (Figure S4). These results suggest that CCR1-mediated cell proliferation exit is tissue-specific.

### The soluble FeA level decreases during leaf development

It has been reported that *ccr1* mutants contain elevated levels of FeA (Derikvand *et al.*, 2008; Vanholme *et al.*, 2012). This prompted us to investigate whether the increased FeA level in the mutants is the reason for the alterations in cell proliferation and causes the other developmental defects. To this end, we first analyzed the soluble FeA level in wild-type leaves at various stages of development by LC-MS, to obtain information about relationships among FeA levels, cell growth states and *CCR1* expression levels. On day 7, leaves contained a considerable amount of soluble FeA, but the FeA level decreased substantially on day 9 and became undetectable by day 11 onwards (Figure 3a). Thus, the decrease in FeA levels is correlated with the increased *CCR1* expression levels, as shown in Figure 2, but negatively correlated with cell division.

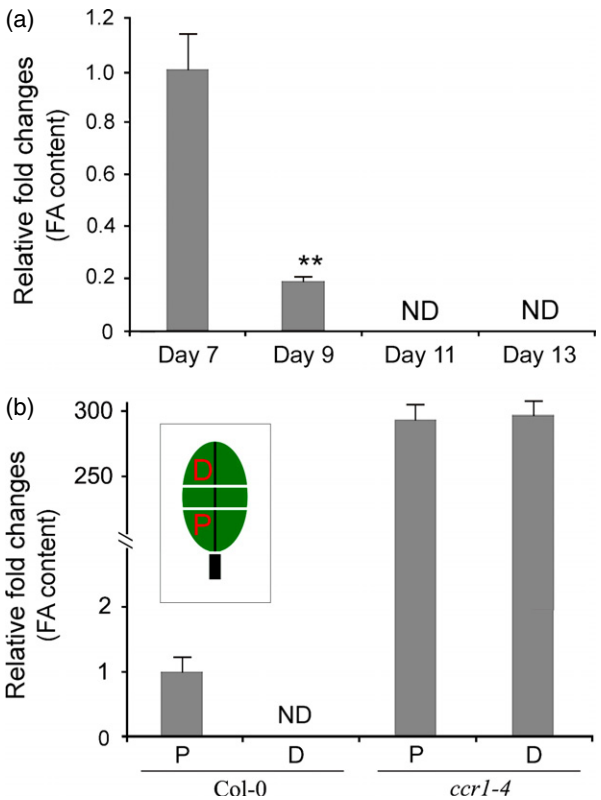


**Figure 3.** Analysis of FeA levels during leaf development.
(a) LC-MS was performed to detect changes in soluble FeA levels during leaf development. The first leaves were analyzed on days 7, 9, 11, and 13.
(b) Measurements of FeA contents from proximal (P) or distal (D) parts of first leaves of wild-type and *ccr1-4* on day 9. The inset shows the leaf parts used in preparing samples for analysis. The value from the proximal part of wild-type leaves was arbitrarily fixed at 1.0.
Values are means and SE of three biological replicates. Asterisks indicate statistically significant differences compared with the value of day-7 leaves (**$P < 0.01$). ND, not detected.

As leaves on day 9 showed *CCR1* expression strongly at the tip, mildly in the middle, and no expression at the proximal regions (Figure 2b), these leaves are suitable for further analysis of the correlation between *CCR1* expression and FeA levels. We thus separated the distal from the proximal parts, removing the middle parts (Figure 3b, inset), and compared the FeA content in the separated distal and proximal parts. In wild-type plants, although the proximal part of the first leaves on day 9 contained soluble FeA, it was not detectable in the distal part (Figure 3b). However, in *ccr1-4* plants, both proximal and distal parts contained substantially increased levels of soluble FeA (Figure 3b). We also analyzed soluble FeA levels in the root, where *CCR1* is strongly expressed, but failed to detect

it (Figure S4). Because the increase in *CCR1* expression levels is closely associated with the decrease in FeA levels, there is the possibility that the effect of CCR1 action on cell proliferation may occur via altered FeA levels in leaves.

### The distribution pattern of ROS resembles the *CCR1* expression pattern in leaves

Because FeA scavenge ROS in solution, in cultured neurons and in synaptosomal systems (Kanski *et al.*, 2002), and oxidative stress terminates cell proliferation (Burdon, 1995; Boonstra and Post, 2004; Guo *et al.*, 2010; Tsukagoshi *et al.*, 2010), we then investigated whether the FeA level was negatively correlated with ROS levels during leaf development. Using the diaminobenzidine (DAB) staining technique, we analyzed the distribution pattern of hydrogen peroxide ($H_2O_2$), a type of ROS, in the first leaf of wild-type and *ccr1-4* plants. In wild-type leaves, the pattern of DAB staining resembled that of *CCR1* expression; it began at the distal part of the leaf on day 7 (Figure 4a), and extended to the middle portion of the leaf by day 9 (Figure 4b), and the entire leaf by day 11 onwards (Figure 4c, d). Compared with wild-type plants, *ccr1-4* showed delayed $H_2O_2$ accumulation in the first leaf on day 7 (Figure 4e), and the staining in leaves on day 9 was associated only with trichomes (Figure 4f). Although leaves of *ccr1-4* showed DAB staining on days 11 and 13 (Figure 4g,h), the staining was much weaker than that in leaves of wild-type plants at the same age.

This $H_2O_2$ accumulation pattern was further confirmed by staining with CM-$H_2$DCFDA [5-(and-6)-chloromethyl-2′,7′-dichlorodi-hydrofluorescein diacetate, acetyl ester] (Jambunathan, 2010). For example, on day 9, there was strong DCF fluorescence at the distal region of the wild-type leaf (Figure 4i–l), but it was very weak in the similar region of the *ccr1-4* leaf (Figure 4m–o). In proximal regions of same-age leaves, DCF fluorescence was barely detected in either wild-type or *ccr1-4* seedlings (Figure 4p–s). As the *ccr1-4* leaves contained increased levels of FeA and decreased levels of $H_2O_2$, and FeA antagonizes ROS, which at a high level are capable of blocking cell proliferation, it is possible that the high FeA level may be the reason for increased cell proliferation in *ccr1* mutants.

### Treatment of plants with FeA and $H_2O_2$ affects cell proliferation

To provide further evidence for the role of FeA, we treated Arabidopsis seedlings with $H_2O_2$ and FeA, and analyzed changes in their growth. Compared with leaves of mock-treated seedlings (Figure 5a), the leaves of seedlings treated with 0.5 and 1 mM $H_2O_2$ had fewer, but larger, palisade cells (Figure 5b,c,e,f). A further increase in $H_2O_2$ concentration to 5 mM not only caused more severe reductions in cell number (Figure 5e), but also decreased the cell size (Figure 5d,f).

Treatments with low concentrations of FeA (50 or 125 μM) increased the number of palisade cells in the leaves, but reduced the cell size (Figure 5g,h,k,l), mimicking the cells in the leaves of the *ccr1-4* mutant. A higher FeA concentration (250 μM) further decreased cell size (Figure 5i,l), but, instead of the increase in cell number caused by treatment with lower concentrations of FeA, the number of cells was decreased (Figure 5k). It is possible that treatment with a high concentration of FeA has some side-effects on cell proliferation. In wild-type leaves treated with both 1 mM $H_2O_2$ and 50 μM FeA, the cell number and cell size appeared normal (Figure 5j,l).

Root cells of young seedlings treated with FeA showed a decrease in endogenous $H_2O_2$ levels. Whereas wild-type roots of 7-day-old seedlings accumulated $H_2O_2$, the CM-$H_2$DCFDA fluorescence was barely detected in *ccr1-4* roots (Figure S5). Treatment of wild-type seedlings with 50 μM FeA markedly reduced the $H_2O_2$ level in the root (Figure S5). As for palisade cells, the number of cortex cells in the root meristematic zone was also increased by the FeA treatment, but decreased by the $H_2O_2$ treatment (Figure S5).

### Reduced FeA levels in plants result in an increase in ROS levels and defective cell proliferation

To obtain further evidence that FeA promotes cell proliferation *in planta*, it is important to identify and characterize plants that contain reduced FeA levels. However, to our knowledge, Arabidopsis mutants with reduced FeA levels have not been reported. In lignin biosynthesis, the last

**Figure 4.** *ccr1-4* has decreased $H_2O_2$ levels in leaves.
(a–d) DAB staining to detect $H_2O_2$ during leaf development. Accumulation of $H_2O_2$ started at the distal part and then expanded to the whole leaf. The first rosette leaves from a wild-type plant on days 7 (a), 9 (b), 11 (c) and 13 (d) are shown.
(e–h) DAB staining of *ccr1-4* leaves on days 7 (e), 9 (f), 11 (g) and 13 (h), showing delayed $H_2O_2$ accumulation.
(i) Illustration of the distal position (red arrow) and proximal position (yellow arrow) at which fluorescence was analyzed by laser scanning confocal microscopy to detect CM-$H_2$DCFDA-stained ROS signals.
(j–o) Detection of ROS by CM-$H_2$DCFDA staining in leaves on day 9. Fluorescence was examined in the distal parts of a wild-type leaf (j–l) or a *ccr1-4* leaf (m–o). (j, m) CM-$H_2$DCFDA signals. (k, n) Chlorophyll autofluorescence. (l, o) Merged images for (j, k) and (m, n), respectively.
(p–s) Fluorescence was examined in the proximal parts of a wild-type leaf (p, q) or a *ccr1-4* leaf (r, s). (p, r) CM-$H_2$DCFDA fluorescence signals were not detected. (q, s) Chlorophyll autofluorescence.
The images for the wild-type leaves (j–l, p, q) and *ccr1-4* leaves (m–o, r, s) are from the same leaves, respectively. Scale bars = 0.25 mm (a, e), 0.5 mm (b, f), 1 mm (c, d, g, h), 20 μm (j) and 40 μm (p). Images in (k–o) are at the same magnification as that in (j). Images in (r) and (s) are at the same magnification as that in (p).

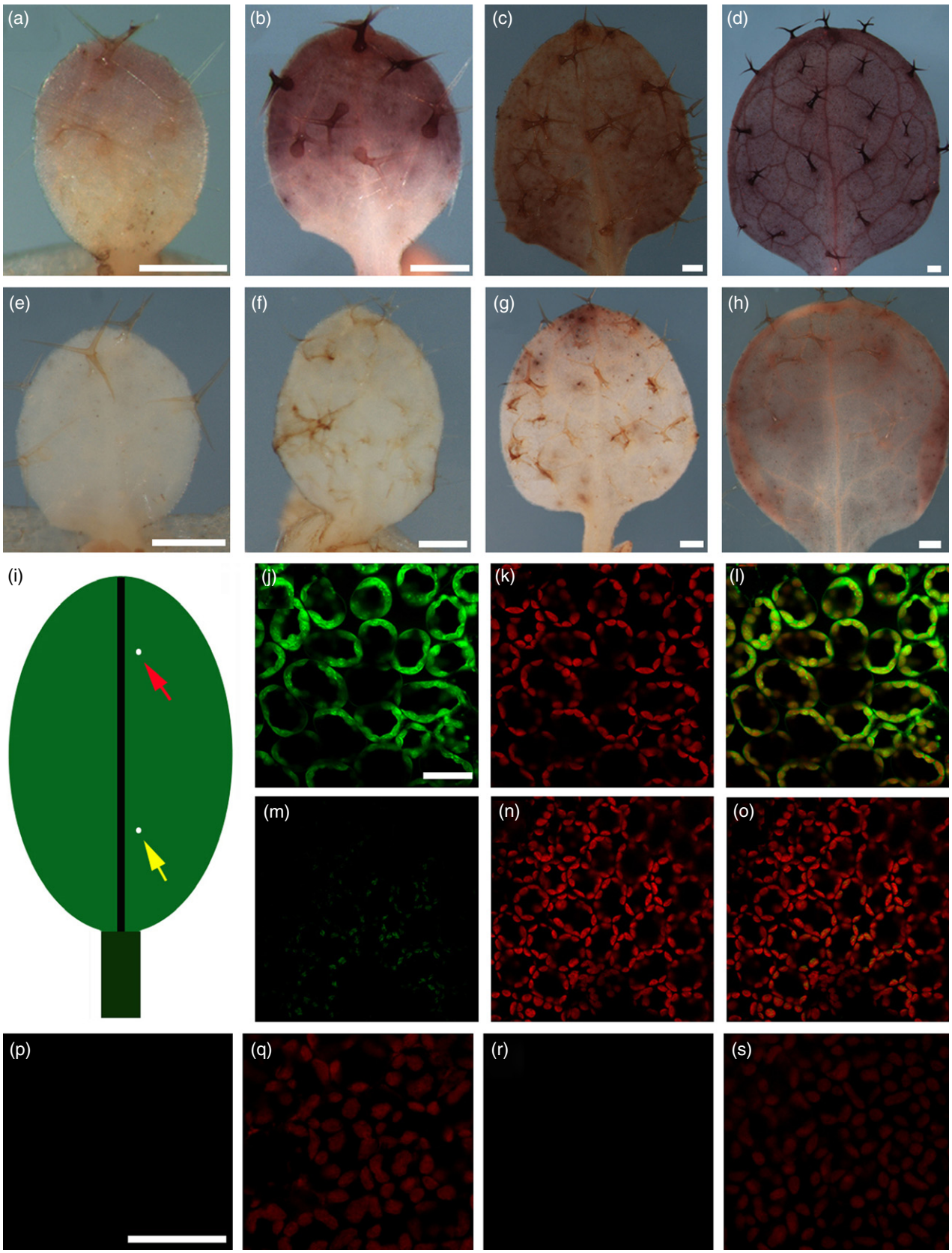


 

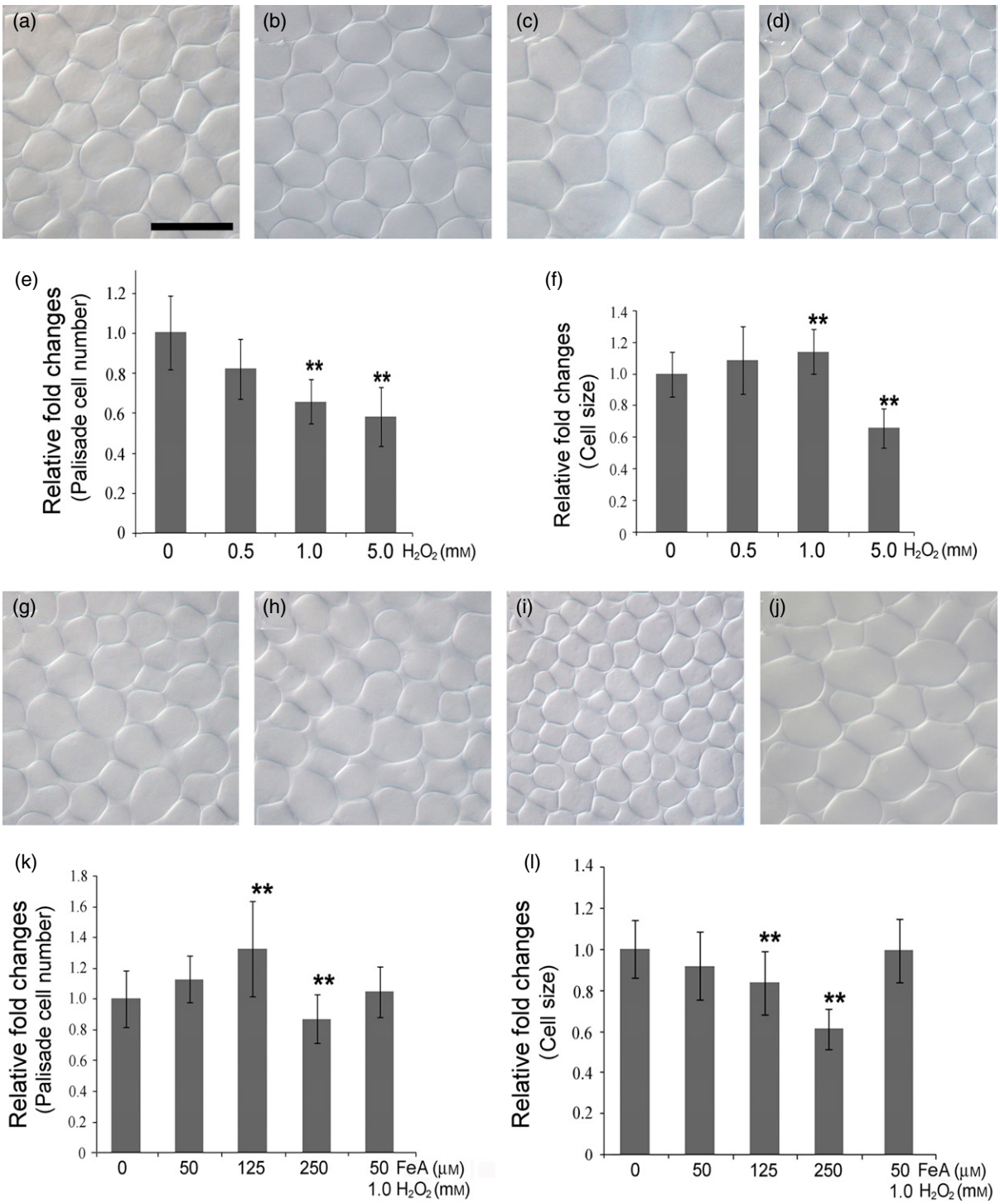


**Figure 5.** Treatment of seedlings with $H_2O_2$ or FeA resulted in changes in the cell number and cell size of leaves.
(a–d) Differential interference contrast microscopy to analyze palisade cells of the first leaves on day 12 from wild-type plants that were mock-treated (a) or on day 5 treated with $H_2O_2$ at the concentrations of 0.5 mM (b), 1.0 mM (c) or 5.0 mM (d).
(e, f) Quantitative analysis of the palisade cell number (e) and size (f) in the first leaves of $H_2O_2$-treated wild-type plants on day 12.
(g–j) Palisade cells of the first rosette leaves from wild-type seedlings on day 12, on day 5 treated with FeA at 50 μM (g), 125 μM (h) or 250 μM (i), or treated with 50 μM FeA and 1 mM $H_2O_2$ (j).
(k, l) Quantitative analysis of the palisade cell number (k) and size (l) from the first leaves of wild-type plants on day 12, treated with FeA or FeA plus $H_2O_2$.
Scale bar, 50 μm in (a). Images in (a–d) and (g–j) are at the same magnification, and photographs were taken at the positions shown in Figure 4(i). Values in (e, f, k, l) are means ± SD ($n$ = 10). The values for samples from mock-treated seedlings were arbitrarily fixed as 1.0. Asterisks indicate statistically significant differences compared with time 0 (**$P$ < 0.01).

three steps in G-type monolignol formation are catalyzed by caffeoyl CoA 3-*O*-methyltransferase (CCoAOMT), CCR1 and CAD-C/CAD-D (Figure 6a) (Boerjan *et al.*, 2003; Vanholme *et al.*, 2010, 2012). In Arabidopsis, CCoAOMT has been shown to be functionally redundant with caffeic acid *O*-methyltransferase (COMT) (Do *et al.*, 2007). Because CCR1 uses feruloyl CoA as the substrate and the *ccr1* mutation results in plants with high levels of FeA, we reasoned that the *comt ccoaomt* double mutant, which is mutated in enzymes that produce feruloyl CoA (Figure 6a), may contain low levels of FeA. We thus first performed an LC-MS analysis to determine FeA levels in *comt ccoaomt*, and found that, on day 7, *comt ccoaomt* leaves contained a much lower FeA level than in wild-type plants (Figure 6b). We also measured the FeA levels of *ccr1-4* and *cad-c cad-d* mutants using leaves on day 7. While the FeA level in *cad-c cad-d* was similar to that in the wild-type, it was dramatically increased in the *ccr1-4* leaves (Figure 6c), consistent with the previous report using stems of the *ccr1-g* mutant (Derikvand *et al.*, 2008). These results indicate that either a lack of FeA or a drastic increase in FeA affects plant growth and development.

To determine whether the *comt ccoaomt* phenotypes are caused by the lack of FeA, we treated *comt ccoaomt* seedlings with FeA in growth medium. Compared with the wild-type (Figure 7a), the mock-treated *comt ccoaomt* double mutant showed a very small plant size (Figure 7b), with an increased level of $H_2O_2$ (Figure 7c). The *comt ccoaomt* phenotypes were mostly, but not fully, rescued by treatment with FeA (Figure 7d–f), indicating that the phenotypes are at least partly caused by the lack of FeA.

To test whether the antioxidant function of FeA rescued *comt ccoaomt* phenotypes, we treated the *comt ccoaomt* double mutant with *N*-acetyl-L-cysteine (NAC), another antioxidant that may be absorbed by plants (Joo *et al.*, 2001). Application of NAC partially rescued the *comt ccoaomt* phenotypes in a dose-dependent manner (Figure 7g–i), although NAC treatments were not as effective as FeA treatments in rescuing the mutant phenotypes (Figure 7j–l). For instance, treatment of *comt ccoaomt* with 1 mM NAC resulted in increases in leaf size (Figure 7j), leaf number (Figure 7k) and the number of cells per leaf (Figure 7l), but these increases were not as large as those in response to FeA treatments. Because treatments with NAC or FeA decreased the $H_2O_2$ concentrations in the *comt ccoaomt* double mutant (Figure 7c), it is possible that oxidative stress contributed to the *comt ccoaomt* phenotypes.

## DISCUSSION

In multicellular organisms, cell proliferation and differentiation are well balanced for normal development, and initiation of cell differentiation is often accompanied by exit

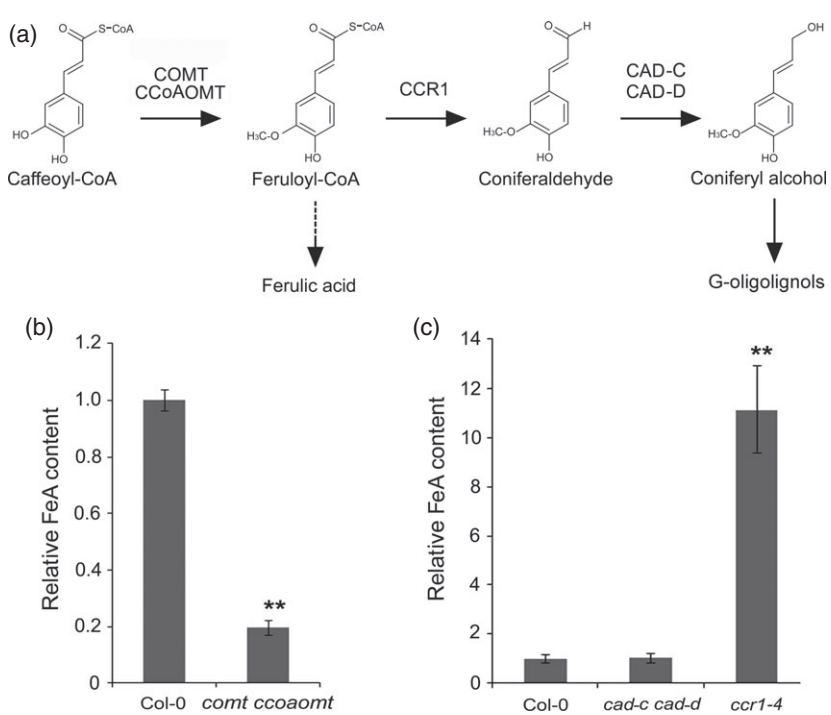


**Figure 6.** Changes of soluble FeA contents in *comt ccoaomt*, *ccr1-4* and *cad-c cad-d* mutants.
(a) The biosynthetic steps from caffeoyl CoA to G-type monolignol. The dashed arrow indicates the proposed step for FeA formation.
(b, c) LC-MS was performed to detect changes in soluble FeA contents in the *comt ccoaomt* double mutant (b), and the *ccr1-4* single mutant and *cad-c cad-d* double mutants (c). Leaves on day 7 were used in the analyses. FeA levels from wild-type Col-0 leaves were arbitrarily fixed at 1.0. Values are means ± SE of three biological replicates. Asterisks indicate statistically significant differences compared with Col-0 (**$P < 0.01$).

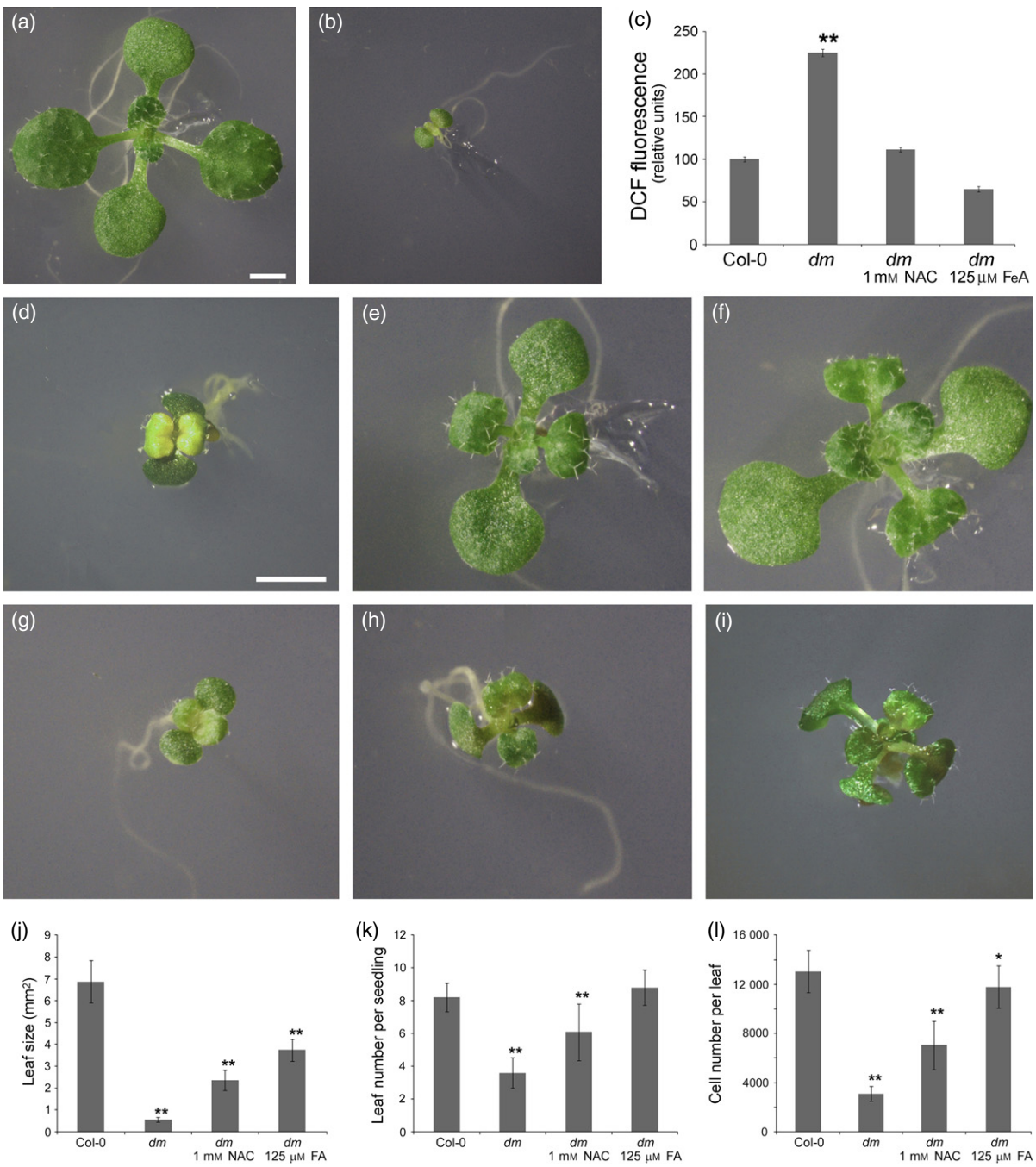


**Figure 7.** The antioxidant function of FeA contributes to the promotion of cell proliferation during plant growth and development.
(a) A 12-day-old wild-type seedling.
(b) A 12-day-old *comt ccoaomt* seedling, showing a dramatically reduced plant size.
Scale bar in (a) = 1 mm. Images in (a) and (b) are at the same magnification.
(c) *comt ccoaomt* double mutant plants contained increased levels of ROS, and treatment with FeA or NAC in growth medium resulted in suppression of ROS levels. Whole seedlings at 12 days old were used in the analyses. Values are means ± SE of three biological replicates. Asterisks indicate statistically significant differences compared with Col-0 (**$P < 0.01$).
(d–f) Phenotypes of the *comt ccoaomt* double mutant were partially rescued by treatment with FeA. Shown are 12-day-old *comt ccoaomt* plants grown on medium containing 25 μM (d), 50 μM (e) or 125 μM (f) FeA.
(g–i) NAC partially rescued the *comt ccoaomt* phenotypes. Shown are 12-day-old *comt ccoaomt* plants, treated in medium containing 0.1 mM (g), 0.5 mM (h) or 1 mM (i) NAC.
Scale bar in (d) = 1 mm. Images in (d–i) are at the same magnification.
(j–l) Quantitative analyses of leaf size (j), leaf numbers per seedling (k), and cell numbers per leaf (l) for *comt ccoaomt* double mutant plants treated with FeA or NAC. Values are means ± SD ($n = 10$). Asterisks indicate statistically significant differences compared with Col-0 (*$P < 0.05$; **$P < 0.01$). *dm*, *comt ccoaomt* double mutant.

from the mitotic cell cycle (Breuer *et al.*, 2010). Thus, control of the cellular transition from the proliferation stage to the differentiation stage is important for plant development. In this study, we showed that activity of CCR1 results in decreased FeA levels. As FeA antagonizes the effect of ROS, and a high level of ROS is associated with exit from the cell cycle in leaves, we propose that ROS may be the previously proposed chloroplast-derived signal (Andriankaja et al., 2012). Thus, CCR1, FeA and ROS may coordinate to direct cell proliferation exit for leaf development. After leaf initiation, the intracellular concentration of soluble FeA peaks because of the limited activity of CCR1, such that leaf cells may retain their rapid proliferation state. During further leaf growth, chloroplasts develop and the activity of the photosynthetic electron transport chain leads to increased ROS levels. Meanwhile, *CCR1* expression increases, and the increased CCR1 activity gradually depletes FeA. The increased activity of ROS terminates the cell cycle and forces leaf cells to enter the differentiation stage. Therefore, CCR1 is an important factor in the process of cell proliferation exit during leaf development.

The role of ROS in leaf development is consistent with that in root development. In roots, ROS is critical for the balance of cell proliferation and differentiation. UPBEAT1 (UPB1), a transcription factor, directly regulates the expression of a set of peroxidases that modulate actions of ROS in the cell proliferation zone and the cell elongation zone where differentiation begins (Tsukagoshi *et al.*, 2010). Our data show that *CCR1* is highly expressed in most cells in the roots, including cells in the zones of cell proliferation. As in leaves, strong expression of *CCR1* depletes the soluble FeA in the root. In contrast to the antioxidant action of FeA in balancing cell proliferation and differentiation in leaves, root-produced FeA may quickly enter the lignin biosynthesis pathway, and thus modulation of ROS in roots probably relies on some other mechanisms.

Our results showed that treatment of seedlings with 50 μM FeA may block the effect of $H_2O_2$ at much higher concentrations. It is possible that the action of FeA against the $H_2O_2$ effect does not occur through a simple ROS depletion process, and FeA may also have a function in strengthening the antioxidant ability of plant cells during ROS stress. This idea is supported by results from an experiment using animal cells: treatment with FeA increased levels of reduced glutathione and a set of antioxidant enzymes in rat hepatocytes (Srinivasan *et al.*, 2006).

Our results show that the cell proliferation stage was dramatically prolonged in *ccr1-4* leaves. The high level of FeA in the *ccr1* mutant may be the reason for the prolonged cell proliferation stage. This possibility is supported by the fact that treatment of Arabidopsis seedlings with FeA increased cell proliferation. The expression of *CCR1* was developmentally regulated; it was barely detected in very young leaves, but showed increased expression during leaf development in regions of the leaf where cell proliferation is about to cease. Coincidently, lignin biosynthesis, which requires CCR1 activity, does not usually occur in highly dividing cells, and thus CCR1 action has two functions for leaf growth and development: termination of cell division and lignin biosynthesis. The regulation of CCR1 activity has been investigated in rice (*Oryza sativa*), and CCR1 was found to be an effector of the Rac small GTPase (Kawasaki, 2006). In future studies, it will be interesting to study the regulation of *CCR1* in more detail. Information on the regulation of *CCR1* expression may greatly increase our understanding of leaf development.

In this study, we have provided evidence that FeA plays important roles in plant growth and development. Recent studies have revealed genetic pathways for lignin biosynthesis. At least ten loci corresponding to key enzymes involved lignin biosynthesis have been identified in Arabidopsis, largely based on characterization of loss-of-function mutants (Vanholme *et al.*, 2012). Although such mutants generally show decreased lignin content, they may grow normally or show dramatic differences in plant growth and development. Here, we analyzed three lignin-reduced mutants with loss-of-function mutations in enzymes catalyzing three consecutive steps of the same pathway. Compared with *cad-c cad-d*, which showed normal growth except for a soft inflorescence stem due to the low lignin content, *ccr1* and *comt ccoaomt* showed very different plant phenotypes. Interestingly, the soluble FeA levels of these three mutants are correlated with their phenotypic severity: *cad-c cad-d* has a similar level of FeA to that in the wild-type, but *comt ccoaomt* and *ccr1* contain either dramatically reduced or increased FeA levels. Based on these results, we propose that normal or dramatically altered levels of certain intermediates in lignin biosynthesis are one reason why lignin-deficient mutants have either normal or severely altered phenotypes.

Plants produce various kinds of antioxidants, and it is possible that each plant-produced antioxidant has a specific role in protecting the cells against ROS. FeA is perhaps the most abundant antioxidant in plant cells. The presence of such an abundant antioxidant in plants may have some significance. Unlike the cells of other living organisms, plant cells contain chloroplasts, which possess a photosynthetic electron transport chain that generates extremely large amounts of ROS. These ROS may damage various biological processes and structures if they are not removed appropriately. Therefore, the large amount of FeA may represent a reservoir of antioxidant to quench ROS. On the other hand, whereas many of the antioxidant compounds in plants must be recycled to restore their antioxidant function (Foyer and Noctor, 2011), FeA is not. After FeA depletes the ROS generated by physiological processes, it can serve as an essential material in the plant cell wall (Jacquet *et al.*, 1995; Saulnier and Thibault, 1999).

## EXPERIMENTAL PROCEDURES

### Plant materials and growth conditions

The Arabidopsis mutants *comt* (Goujon *et al.*, 2003), *ccoaomt* (Do *et al.*, 2007), *ccr1-g* (Derikvand *et al.*, 2008) and *cad-c cad-d* (Sibout, 2005) are in the Col-0 background, while *ae7* is in the L*er* background. The double mutant *comt ccoaomt* was constructed by crossing *comt* with *ccoaomt*, and the *comt ccoaomt* double mutant was obtained from segregating $F_2$ progeny, with phenotypes similar to those previously described (Do *et al.*, 2007). For generation of the *ae7* suppressor, approximately 5000 *ae7* seeds were mutagenized using ethyl methanesulfonate and screened. Growth of Arabidopsis was performed as described previously (Chen *et al.*, 2000). For Arabidopsis seedlings grown on plates, surface-sterilized seeds were germinated in half-strength Murashige and Skoog (MS) medium supplemented with 1% sucrose for 5 days, and seedlings were moved to medium containing various chemicals for various times as described in Results.

### Histology and microscopy

The *CCR1*$_{pro}$*:CCR1-GUS* fusion was constructed by PCR amplification of the *CCR1* gene including 1 kb of promoter and 3 kb of transcribing regions, using primers 5′-GCAGCGAAAGAGCCAACGGC-3′ and 5′-CGGATCCTGCCATCAGTTACCTTGTCCTCCGT-3′. After sequence verification, the *CCR1*$_{pro}$*:CCR1* fragment was inserted into the binary vector p1300 (http://www.cambia.org/daisy/cambia/585), upstream to and in-frame with the GUS reporter gene. Plant transformation, GUS staining of seedlings or organs for GUS-expressing transgenic plants, light dissecting microscopy and differential interference contrast microscopy were performed as described previously (Li *et al.*, 2005; Yuan *et al.*, 2010).

### Flow cytometric analyses

Flow cytometric analyses were performed as described previously (Yuan *et al.*, 2010). Briefly, the first leaves were harvested from 9 to 26-day-old seedlings, chopped with a razor blade in a Petri dish containing 1 ml nuclear isolation and stain buffer (NIM-DAPI 10; Beckman Coulter, http://www.beckmancoulter.com), and then filtered twice through a 40 μm mesh. The isolated nuclei were analyzed using a MoFlo XDP flow cytometer (Beckman Coulter).

### Measurements of cell numbers and leaves

For measurement of leaf size, seeds were grown on plates that were placed vertically. At 7 days after germination, seedlings were moved to new plates containing various chemicals for an additional 5 days. Images were first obtained by light dissecting microscopy for leaves, and the leaf size was then analyzed using ImageJ software (http://rsb.info.nih.gov/ij/). For measurement of cell size, fresh leaves were treated overnight with chloral solution (chloral hydrate/glycerol/water, 8:2:1 v/v/v) (Tsuge *et al.*, 1996). Photographs were obtained by differential interference contrast microscopy for cleared leaves at the positions shown in Figure 4(i), and the sizes of all cells from each image were further analyzed using ImageJ software. The number of cells per leaf was determined as the mean leaf size divided by the mean cell size. For analysis of roots, we used 7-day-old seedlings grown on half-strength MS plates with or without chemical treatment. Measurements of root cortex cell numbers were performed as described previously (Hennig and Köhler, 2010). Briefly, roots were dipped in 0.1 μg $\mu l^{-1}$ propidium iodide solution for 1 min, washed three times at room temperature with each for 1 min water, and analyzed by a confocal laser scanning microscope. Images of the root meristematic zone were used to assess cell number. For simplicity, relative fold changes were used to compare cell numbers in the leaf and root, unless otherwise indicated.

### Analysis of ROS in plant organs

3′3-diaminobenzidine (DAB) straining to determine $H_2O_2$ in leaves was performed as described previously (Thordal-Christensen *et al.*, 1997), with the concentration of DAB staining solution at 10 mg $ml^{-1}$. $H_2$DCFDA staining of leaves was performed as described by Yao and Greenberg (2006), with the concentration of staining solution at 10 μM. Quantitative analysis of $H_2O_2$ was performed as described previously (Babu *et al.*, 2003). DCF fluorescence was measured using supernatants from leaf homogenates. The value of the fluorescence intensity of samples prepared from wild-type Col-0 leaves was arbitrarily fixed as 100 units.

### LC-MS analyses

LC-MS was performed as described previously (Derikvand *et al.*, 2008) with modifications. Briefly, leaves of various developmental stages were extracted using 0.2 ml of 80% methanol. The extracts were filtered through a 0.22 μm mesh before LC-MS analysis.

## ACKNOWLEDGEMENTS

We thank L. Jouanin (INRA Centre de Versailles-Grignon), the European Arabidopsis Stock Center (http://arabidopsis.info/), and the Arabidopsis Biological Resource Center (https://abrc.osu.edu/) for mutant seeds. P. Doerner (School of Biological Sciences, University of Edinburgh) for the *CYCB1;1*$_{pro}$*:Dbox-GUS/Col-0* seeds, and L. Xu (Shanghai Institute of Plant Physiology and Ecology) and J. Balk (Department of Biological Chemistry, John Innes Centre) for useful discussions. This work was supported by a grant from the National Basic Research Program of China (973 Program, 2012CB910503).

## SUPPORTING INFORMATION

Additional Supporting Information may be found in the online version of this article.

**Figure S1.** Identification of an *ae7* suppressor mutant.

**Figure S2.** Molecular identification of the *CCR1* gene.

**Figure S3.** Cell size and cell number per leaf for the *ccr1-g* mutant.

**Figure S4.** Expression patterns of *CCR1* in the root.

**Figure S5.** Effects of FeA and $H_2O_2$ on cell numbers in the cortex of the root meristematic zone.

## REFERENCES

**Anastasiou, E., Kenz, S., Gerstung, M., MacLean, D., Timmer, J., Fleck, C. and Lenhard, M.** (2007) Control of plant organ size by KLUH/CYP78A5-dependent intercellular signaling. *Dev. Cell*, **13**, 843–856.

**Andriankaja, M., Dhondt, S., De Bodt, S. *et al.*** (2012) Exit from proliferation during leaf development in *Arabidopsis thaliana*: a not-so-gradual process. *Dev. Cell*, **22**, 64–78.

**Babu, T.S., Akhtar, T.A., Lampi, M.A., Tripuranthakam, S., Dixon, D.G. and Greenberg, B.M.** (2003) Similar stress responses are elicited by copper and ultraviolet radiation in the aquatic plant *Lemna gibba*: implication of reactive oxygen species as common signals. *Plant Cell Physiol.* **44**, 1320–1329.

**Beemster, G.T., Mironov, V. and Inze, D.** (2005) Tuning the cell-cycle engine for improved plant performance. *Curr. Opin. Biotechnol.* **16**, 142–146.

**Boerjan, W., Ralph, J. and Baucher, M.** (2003) Lignin biosynthesis. *Annu. Rev. Plant Biol.* **54**, 519–546.

**Boonstra, J. and Post, J.A.** (2004) Molecular events associated with reactive oxygen species and cell cycle progression in mammalian cells. *Gene*, **337**, 1–13.

**Breuer, C., Ishida, T. and Sugimoto, K.** (2010) Developmental control of endocycles and cell growth in plants. *Curr. Opin. Plant Biol.* **13**, 654–660.

**Burdon, R.H.** (1995) Superoxide and hydrogen peroxide in relation to mammalian cell proliferation. *Free Radic. Biol. Med.* **18**, 775–794.

**Chen, C.B., Wang, S.P. and Huang, H.** (2000) LEUNIG has multiple functions in gynoecium development in Arabidopsis. *Genesis*, **26**, 42–54.

**Derikvand, M., Sierra, J.B., Ruel, K., Pollet, B., Do, C.-T., Thévenin, J., Buffard, D., Jouanin, L. and Lapierre, C.** (2008) Redirection of the phenylpropanoid pathway to feruloyl malate in *Arabidopsis* mutants deficient for cinnamoyl-CoA reductase 1. *Planta*, **227**, 943–956.

**Dewitte, W. and Murray, J.A.** (2003) The plant cell cycle. *Annu. Rev. Plant Biol.* **54**, 235–264.

**Do, C.T., Pollet, B., Thévenin, J., Sibout, R., Denoue, D., Barrière, Y., Lapierre, C. and Jouanin, L.** (2007) Both caffeoyl coenzyme A 3-O-methyltransferase 1 and caffeic acid O-methyltransferase 1 are involved in redundant functions for lignin, flavonoids and sinapoyl malate biosynthesis in Arabidopsis. *Planta*, **226**, 1117–1129.

**Donnelly, P.M., Bonetta, D., Tsukaya, H., Dengler, R.E. and Dengler, N.G.** (1999) Cell cycling and cell enlargement in developing leaves of Arabidopsis. *Dev. Biol.* **215**, 407–419.

**Efroni, I., Eshed, Y. and Lifschitz, E.** (2010) Morphogenesis of simple and compound leaves: a critical review. *Plant Cell*, **22**, 1019–1032.

**Foyer, C.H. and Noctor, G.** (2011) Ascorbate and glutathione: the heart of the redox hub. *Plant Physiol.* **155**, 2–18.

**Foyer, C.H. and Shigeoka, S.** (2011) Understanding oxidative stress and antioxidant functions to enhance photosynthesis. *Plant Physiol.* **155**, 93–100.

**Goffner, D., Campbell, M.M., Campargue, C., Clastre, M., Borderies, G., Boudet, A. and Boudet, A.M.** (1994) Purification and characterization of cinnamoyl coenzyme A:NADP oxidoreductase in *Eucalyptus gunnii*. *Plant Physiol.* **106**, 625–632.

**Goujon, T., Sibout, R., Pollet, B. *et al.*** (2003) A new *Arabidopsis thaliana* mutant deficient in the expression of O-methyltransferase impacts lignins and sinapoyl esters. *Plant Mol. Biol.* **51**, 973–989.

**Graf, E.** (1992) Antioxidant potential of ferulic acid. *Free Radic. Biol. Med.* **13**, 435–448.

**Granier, C. and Tardieu, F.** (2009) Multi-scale phenotyping of leaf expansion in response to environmental changes: the whole is more than the sum of parts. *Plant, Cell Environ.* **32**, 1175–1184.

**Guo, Y.L., Chakraborty, S., Rajan, S.S., Wang, R. and Huang, F.** (2010) Effects of oxidative stress on mouse embryonic stem cell proliferation, apoptosis, senescence, and self-renewal. *Stem Cells Dev.* **19**, 1321–1331.

**Hennig, L. and Köhler, C.** (2010) *Plant Developmental Biology: Methods and Protocols*. New York, NY: Humana.

**Jacqmard, A., De Veylder, L., Segers, G., Engler, J.D., Bernier, G., Van Montagu, M. and Inze, D.** (1999) Expression of CKS1At in *Arabidopsis thaliana* indicates a role for the protein in both the mitotic and the endoreduplication cycle. *Planta*, **207**, 496–504.

**Jacquet, G., Pollet, B. and Lapierre, C.** (1995) New ether-linked ferulic acid-coniferyl alcohol dimers identified in grass straws. *J. Agr. Food Chem.* **43**, 2746–2751.

**Jambunathan, N.** (2010) Determination and detection of reactive oxygen species (ROS), lipid peroxidation, and electrolyte leakage in plants. In *Plant Stress Tolerance*. (Sunkar, R., ed). Totowa, NJ: Humana Press, pp. 291–297.

**Jones, L., Ennos, A.R. and Turner, S.R.** (2001) Cloning and characterization of *irregular xylem4* (*irx4*): a severely lignin-deficient mutant of Arabidopsis. *Plant J.* **26**, 205–216.

**Joo, J.H., Bae, Y.S. and Lee, J.S.** (2001) Role of auxin-induced reactive oxygen species in root gravitropism. *Plant Physiol.* **126**, 1055–1060.

**Kanski, J., Aksenova, M., Stoyanova, A. and Butterfield, D.A.** (2002) Ferulic acid antioxidant protection against hydroxyl and peroxyl radical oxidation in synaptosomal and neuronal cell culture systems in vitro: structure-activity studies. *J. Nutr. Biochem.* **13**, 273–281.

**Kawasaki, T.** (2006) Cinnamoyl-CoA reductase, a key enzyme in lignin biosynthesis, is an effector of small GTPase Rac in defense signaling in rice. *Proc. Natl Acad. Sci. USA*, **103**, 230–235.

**Kazama, T., Ichihashi, Y., Murata, S. and Tsukaya, H.** (2010) The mechanism of cell cycle arrest front progression explained by a KLUH/CYP78A5-dependent mobile growth factor in developing leaves of Arabidopsis thaliana. *Plant Cell Physiol.* **51**, 1046–1054.

**Lacombe, E., Hawkins, S., VanDoorsselaere, J., Piquemal, J., Goffner, D., Poeydomenge, O., Boudet, A.M. and GrimaPettenati, J.** (1997) Cinnamoyl CoA reductase, the first committed enzyme of the lignin branch biosynthetic pathway: cloning, expression and phylogenetic relationships. *Plant J.* **11**, 429–441.

**Li, H., Xu, L., Wang, H., Yuan, Z., Cao, X.F., Yang, Z.N., Zhang, D.B., Xu, Y.Q. and Huang, H.** (2005) The putative RNA-dependent RNA polymerase *RDR6* acts synergistically with *ASYMMETRIC LEAVES1* and *2* to repress *BREVIPEDICELLUS* and MicroRNA165/166 in Arabidopsis leaf development. *Plant Cell*, **17**, 2157–2171.

**Luderitz, T. and Grisebach, H.** (1981) Enzymic synthesis of lignin precursors. Comparison of cinnamoyl-CoA reductase and cinnamyl alcohol:NADP+ dehydrogenase from spruce (*Picea abies* L.) and soybean (*Glycine max* L.). *Eur. J. Biochem.* **119**, 115–124.

**Luo, D., Bernard, D.G., Balk, J., Huang, H. and Cui, X.** (2012) The DUF59 family gene *AE7* acts in the cytosolic iron-sulfur cluster assembly pathway to maintain nuclear genome integrity in Arabidopsis. *Plant Cell*, **24**, 4135–4148.

**Piquemal, J., Lapierre, C., Myton, K., O'Connell, A., Schuch, W., Grima-Pettenati, J. and Boudet, A.M.** (1998) Down-regulation of cinnamoyl-CoA reductase induces significant changes of lignin profiles in transgenic tobacco plants. *Plant J.* **13**, 71–83.

**Poethig, R.S. and Sussex, I.M.** (1985) The developmental morphology and growth dynamics of the tobacco leaf. *Planta*, **165**, 158–169.

**Pyke, K.A. and Leech, R.M.** (1991) Rapid image analysis screening procedure for identifying chloroplast number mutants in mesophyll cells of *Arabidopsis thaliana* (L.) Heynh. *Plant Physiol.* **96**, 1193–1195.

**Saulnier, L. and Thibault, J.F.** (1999) Ferulic acid and diferulic acids as components of sugar-beet pectins and maize bran heteroxylans. *J. Sci. Food Agric.* **79**, 396–402.

**Sibout, R.** (2005) *CINNAMYL ALCOHOL DEHYDROGENASE-C and -D* are the primary genes involved in lignin biosynthesis in the floral stem of *Arabidopsis*. *Plant Cell*, **17**, 2059–2076.

**Srinivasan, M., Sudheer, A.R., Pillai, K.R., Kumar, P.R., Sudhakaran, P.R. and Menon, V.P.** (2006) Influence of ferulic acid on γ-radiation induced DNA damage, lipid peroxidation and antioxidant status in primary culture of isolated rat hepatocytes. *Toxicology*, **228**, 249–258.

**Thevenin, J., Pollet, B., Letarnec, B., Saulnier, L., Gissot, L., Maia-Grondard, A., Lapierre, C. and Jouanin, L.** (2010) The simultaneous repression of CCR and CAD, two enzymes of the lignin biosynthetic pathway, results in sterility and dwarfism in *Arabidopsis thaliana*. *Mol. Plant*, **4**, 70–82.

**Thordal-Christensen, H., Zhang, Z.G., Wei, Y.D. and Collinge, D.B.** (1997) Subcellular localization of $H_2O_2$ in plants. $H_2O_2$ accumulation in papillae and hypersensitive response during the barley-powdery mildew interaction. *Plant J.* **11**, 1187–1194.

**Tsuge, T., Tsukaya, H. and Uchimiya, H.** (1996) Two independent and polarized processes of cell elongation regulate leaf blade expansion in *Arabidopsis thaliana* (L.) Heynh. *Development*, **122**, 1589–1600.

**Tsukagoshi, H., Busch, W. and Benfey, P.N.** (2010) Transcriptional regulation of ROS controls transition from proliferation to differentiation in the root. *Cell*, **143**, 606–616.

**Vanholme, R., Demedts, B., Morreel, K., Ralph, J. and Boerjan, W.** (2010) Lignin biosynthesis and structure. *Plant Physiol.* **153**, 895–905.

**Vanholme, R., Storme, V., Vanholme, B., Sundin, L., Christensen, J.H., Goeminne, G., Halpin, C., Rohde, A., Morreel, K. and Boerjan, W.** (2012) A systems biology view of responses to lignin biosynthesis perturbations in Arabidopsis. *Plant Cell*, **24**, 3506–3529.

**Yao, N. and Greenberg, J.T.** (2006) Arabidopsis ACCELERATED CELL DEATH2 modulates programmed cell death. *Plant Cell*, **18**, 397–411.

**Yuan, Z., Luo, D., Li, G., Yao, X., Wang, H., Zeng, M., Huang, H. and Cui, X.** (2010) Characterization of the *AE7* gene in Arabidopsis suggests that normal cell proliferation is essential for leaf polarity establishment. *Plant J.* **64**, 331–342.

 